

Site-specific presentation of single recombinant proteins in defined nanoarrays

Tobias Wolfram, Ferdinand Belz, Tobias Schoen, and Joachim P. Spatz^{a)}

Department of New Materials and Biosystems, Max-Planck-Institute for Metals Research, Heisenbergstr. 3, D-70569 Stuttgart, Germany; Department of Biophysical Chemistry, University of Heidelberg, Heisenbergstr. 3, D-70569 Stuttgart, Germany; and Institute for Molecular Biophysics, The Jackson Laboratory, 600 Main Street, Bar Harbor, Maine 04609

(Received 22 December 2006; accepted 9 February 2007; published 29 March 2007)

The authors describe the deposition of single biomolecules on substrates at defined spacing by pure self-assembly. The substrate is equipped with an array of 8 nm large gold particles which form the template for biomolecule binding. The authors verified the successful binding of single biomolecules via specific antibody labeling and imaging by fluorescence microscopy. Scanning force microscopy provided evidence that every gold nanoparticle of the pattern is occupied by at least one biomolecule. Furthermore, gold conjugated secondary antibodies in combination with scanning electron microscopy proved that at least 75% of the nanoparticles carried only one active biomolecule. The precision given by such surface densities is molecularly defined and such considerably higher than in any other case reported so far. © 2007 American Vacuum Society. [DOI: 10.1116/1.2713991]

I. INTRODUCTION

Immobilization of biomolecules on glass cover slips by a variety of methods is widely applied in cell biology considering the study of cellular responses on surfaces presenting biomolecules.¹ Available surface functionalization methods lack a proper control of the amount of proteins which is immobilized to the surface on the scale of single proteins, i.e., presenting protein surface concentrations with molecular precision. In general, global biomolecule surface densities are evaluated by, e.g., x-ray photoelectron spectroscopy, infrared spectroscopy, UV-visible absorption, fluorescence intensity, or radioactive labeling. However, global protein surface density lacks information on molecule-to-molecule distance. In order to consider functions given by multivalent interactions between proteins,² it is of great importance not only to control the global but molecularly defined surface density, i.e., protein-protein spacing. In particular, cell signal transduction due to receptor clustering is drastically affected by molecularly defined surface densities.^{3,4}

As well as density, orientation of biomolecules at interfaces also influences the activity of biofunctionalized interfaces. Orientation of proteins according to their *N* and *C* terminus is realized by a variety of tags such as biotin, cysteine, or histidine tag (His tag).⁵ Conventional streptavidin or avidin presents four binding sites for biotin and therefore lacks the possibility to immobilize single biotin conjugated proteins.^{6,7} Recently, a monovalent streptavidin-biotin system was reported.⁸ The binding state of biotin-streptavidin cannot be easily regulated and displays a rather strong affinity. Metal-coordinating groups such as nitrilotriacetic acid^{9–11} (NTA) allow immobilization of single proteins with His tag by Ni²⁺ chelators. Its binding state is regulated by ethylene-

diamine tetra-acetic acid or other chelating agents. This system has a K_D of 10^{-13} which displays a higher binding activity than most monoclonal antibodies and other tag systems.^{12,13} Binding strength is enhanced by multivalent binding concepts¹⁴ and TACN-tag systems,¹⁵ offering much stronger affinities than conventional NTA. However, once immobilized on homogeneous surfaces all of these systems lack an appropriate spatial control, i.e., spacing of individual molecules at interfaces.

Laterally confined molecule presentation at interfaces was limited to submicrometer patches, due to technological limitations.⁹ Even smaller two-dimensional structures with <100 nm feature sizes could be prepared by nanoimprint lithography.¹⁶ By developing micellar nanolithography, this resolution limit was reduced to structures <10 nm. So far, only small peptides were immobilized on those substrates.^{3,4} Peptides alone can induce certain cell biological relevant processes, such as focal adhesions.³ Even more complex recruitment processes in the cell membrane such as in cholesterol enriched domains¹⁷ and synapses¹⁸ desire the activation through proteins in defined pattern. However, addressing questions in cell biology with respect to molecular spacing generates an important need for defined nanostructured surfaces which are capable to accept only a single molecule at an individual binding site in a defined orientation.^{19,20}

II. EXPERIMENT

For protein immobilization studies quasihexagonally arranged gold nanopatterns on glass surfaces were prepared as described previously in Ref. 3. Gold nanoparticles had a diameter of approximately 6 nm and a lateral spacing of 30, 96, or 160 nm. To prevent nonspecific protein interactions with glass, a monomolecular film of mPEG-triethoxysilanes were covalently bound to the glass surface. The hydrophilic glass or silicon substrates were inserted for 16–20 h in a

^{a)}Author to whom correspondence should be addressed; electronic mail: joachim.spatz@urz.uni-heidelberg.de

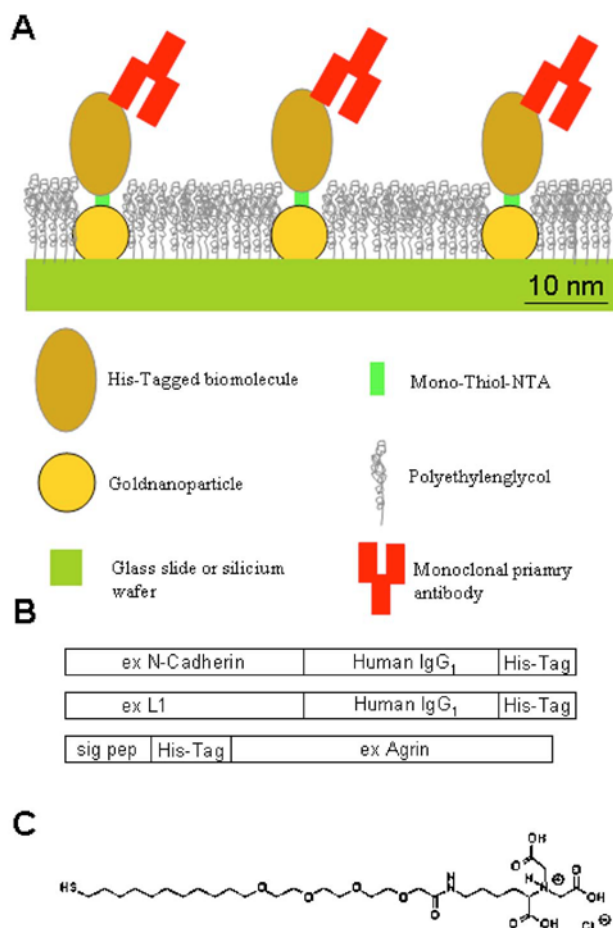


FIG. 1. (a) Scheme of the gold nanopattern and biomolecule presentation at a surface; (b) biomolecules used in this study: N-cadherin, L1, and agrin are all expressed with a His tag; (c) mono-NTA-thiol linker.

flask containing a 0.25 mM toluene (p.a., dried over molecular sieve; pore size: 3 Å, EMD) mPEG2000-urea solution. After adding 2.5 μM triethylamine (EMD) the flask was heated to 80 °C. All chemicals were stored and processed under inert gas atmosphere of either nitrogen (quality 5.0) or argon (quality 5.0) (Advantage Gases, Bangor, USA). In order to remove the physisorbed polyethyleneglycol (PEG) residues, the samples were rinsed with ethyl acetate (p.a., EMD) and treated for 2 min in an ultrasound bath, where after samples were again rinsed with ethyl acetate. In a final step, the samples were rinsed with methanol (p.a., EMD), dried under a nitrogen stream, and directly used for the subsequent coupling of biomolecules to the gold nanoparticles. Then, gold nanopatterns were functionalized by mono-NTA-thiols (Prochimia). A stock solution of NTA was diluted to a 1 mM working solution in p.a. ethanol and incubated for 4 h. After washing with HBSS, NiCl₂ was applied on surfaces. After two additional washing steps biomolecules (R&D systems), as schematically shown in Fig. 1(a), were immobilized to NTA-Ni²⁺ complexes.

NTA-thiol functionalized gold dot nanostructures were incubated overnight at 4 °C with 1 μg/ml proteins in phosphate buffer solution (PBS), pH 7.4. After brief washing with

PBS, bound proteins were incubated with monoclonal antibodies (mouse anti-agrin, Stressgen; mouse anti-N-cadherin, Abcam; mouse anti-L1, Cymbus Biotechnology). All bound primary mouse antibodies were stained with secondary anti-mouse conjugated with the fluorescent molecule TRITC (Sigma). Samples were examined with a DMRE microscope (Leica) and a 20×, 0.7 numerical aperture, air PL APO objective. Images were acquired with a Micromax (Princeton Instruments) camera and METAMORPH imaging software (Universal Imaging). Experiments were repeated three times.

Gold nanopattern functionalized with and without N-cadherin are analyzed by scanning force (SF) microscopy (XE100 AFM, PSIA Corp., Korea) after drying the substrates in nitrogen gas flow. Rotated monolithic silicon tips with symmetric shape and a 30 nm aluminum reflex coating (BudgetSensors, Bulgaria), which have a length 450 μm and a width of 50 μm with a tip radius <10 nm, were utilized. Measurements were taken in contact mode in air under standard conditions (room temperature: 1013 mbars). Three independent experiments were performed for each substrate.

In order to prove the functionality and the number of immobilized biomolecules per single gold nanoparticle, scanning electron microscopy (Zeiss Ultra) in combination with specific immunogold labeling of antibodies was applied. We prepared gold nanoparticle substrates with a 96 ± 12 nm spacing on silicon wafer and biofunctionalized these structures with agrin or N-cadherin. Substrates were incubated for 2 h at room temperature with monoclonal primary antibodies. Ideally, one monoclonal antibody recognizes one binding site per biomolecule. Agrin itself is a monomer offering only one binding site while N-cadherin is a homodimer offering two binding sites. Substrates with monoclonal antibodies were incubated for 1 h at room temperature with gold conjugated secondary antibodies (Jackson ImmunoResearch). After secondary antibody incubation, substrates were washed in PBS and finally in water. Finally, samples were blow dried with nitrogen and sputter coated (BAL-TEC) with a carbon layer. Experiments were repeated three times and for statistical analysis, 830 gold dots for agrin and 1041 for N-cadherin were counted.

III. RESULTS AND DISCUSSION

In this study we present a technology for the positioning of single genetically engineered biomolecules in nanopatterns at interfaces such as glass cover slips and demonstrate a molecularly defined biomolecule density. Figure 1(a) presents the principle experimental concept. Nanostructured gold dot patterns were prepared by micellar diblock copolymer lithography as described previously.^{21,22} It results in the organization of individual gold nanoclusters with a defined and controllable diameter between 1 and 15 nm and lateral spacing between 15 and 250 nm at surfaces by dip coating. Each gold cluster represents a size which makes it a candidate for potentially only immobilizing a single molecule. The lateral spacing between individual gold nanoclusters spans molecularly relevant distances which are also found in protein clusters in cell membranes. Nonspecific binding of mol-

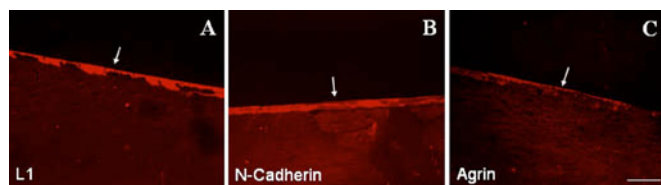


FIG. 2. Fluorescence microscopy of (a) L1, (b) N-cadherin, and (c) agrin immobilized on functionalized gold nanopattern (30 nm spacing of 8 nm large gold particles). Depicted is the boundary (white arrow) which separates the nanopattern area from the pure PEG passivated glass surface. Scale bar is 50 μm for all images.

ecules or proteins to glass cover slips decorated with gold nanopattern is limited by the so-called passivation of the gold free surface area with PEG.³ Three different biomolecules were used in this study [Fig. 1(b)]. L1 is a member of the immunoglobulin superfamily (Ig-SF) and is predominantly expressed in neuronal tissue, mediating cell-cell adhesion.²³ Agrin is a heparan sulfate proteoglycan and is expressed in a variety of different tissues and cell types playing different roles in cellular differentiation.²⁴ N-cadherin is a classical type I cadherin and among other functions mediates calcium dependent cell-cell adhesion in organisms.²⁵ All three biomolecules are expressed as transmembrane proteins. The biomolecules used in this study comprise the extracellular domain for L1, N-cadherin, and the very C-terminal sequence for agrin. L1 and N-cadherin form homodimeric molecules due to an expression sequence of a part of a human IgG1 antibody in the recombinant protein. Furthermore, all biomolecules were expressed as 6 \times -histidine tagged fusion proteins. Agrin is labeled by a His tag at the N terminus, while L1 and N-cadherin expressed the His tag at the C terminus. This tag allows a site directed bioconjugation to the nanogold dots since these are functionalized by monothiol NTA linker [Prochimia, Fig. 1(c)]. This only allows binding of L1 and N-cadherin via the C terminus and agrin via the N terminus to the gold dot surface by NTA-Ni²⁺ chelators. This orientation resembles the natural orientation of these proteins in the cell membrane.

The protein immobilization on nanopatterned areas could be confirmed on a global scale by fluorescent secondary antibodies that bind to the corresponding monoclonal antibodies of the biomolecule [schematically shown in Figure 1(a)] in combination with fluorescence optical microscopy (Leica). Fluorescence microscopy specifically detected fluorescence only from the gold nanopattern and protein functionalized glass surface, as shown in Figs. 2(a)–2(c), bottom area. Here, with each sample the dipping edge which is the boundary between the nanopattern and nonpattern glass surface areas is shown. The nonpattern surface areas do not show any fluorescence. The area of the nanopattern close to the dipping boundary usually shows less uniform and more intense fluorescence due to less ordered and denser packed gold nanopattern.

While fluorescence microscopy gives information on a global length scale with respect to the size of individual molecules or nanostructures, SF and scanning electron (SE) mi-

croscopies may provide local information on successful site-specific functionalization. Figure 3(a) shows a typical SF micrograph of a gold nanopattern surface, where the glass was passivated by PEG and the gold nanoparticles were functionalized by NTA but with no biomolecules. The respective height plots of the lines shown in the image are given in Figs. 3(b) and 3(c). The heights of the gold dots are around 5 ± 0.5 nm. Consideration of an original gold dot height of ~ 8 nm and a PEG layer of 3 nm covering the glass area in between the gold dots confirms the experimental data given. Figure 3(d) shows a typical SF micrograph of an N-cadherin functionalized nanopattern. The N-cadherin biofunctionalized gold dots show a significant increase in height between 12 and 22 nm as indicated by the height plots in Figs. 3(e) and 3(f). The extracellular domain of N-cadherin has a reported length of around 20–25 nm in its outstretched and physiologically active form.²⁶ Taking into account that the proteins were imaged in their dry state the SF data shown in Fig. 3 indicate that each gold dot must be successfully functionalized by at least one biomolecule. Nonfunctionalized gold dots were not found for the areas imaged.

In order to prove the functionality and the number of biomolecules per single gold nanoparticle, scanning electron microscopy in combination with immunogold labeling was applied. Figure 4(a) shows a representative SE micrograph of gold nanopattern biofunctionalized with N-cadherin after incubation with the gold labeled secondary antibody only, without incubation of primary antibodies. The white dots represent the gold from the nanopattern comparable to a situation where gold dots are not functionalized by biomolecules. The gold nanoparticles have a diameter of approximately 8 nm. Similar results were found for agrin (data not shown). No gold conjugated antibodies were observed, which indicates that unspecific binding of gold conjugated antibodies did not occur at the concentrations applied. Also on the pure PEG passivated surface area no unspecifically adsorbed gold conjugated antibody was found. The situation is very different if the biomolecule functionalized nanostructures were first incubated with the primary antibodies and then with the gold conjugated secondary antibodies, as given in Fig. 4(b) for N-cadherin and in Fig. 4(c) for agrin. In the case of N-cadherin 1041 individual Au nanoparticles of the pattern were analyzed from which 75% were found to be labeled with one (48%) or two (27%) additional gold particles via secondary antibodies at a distance less than 20 nm from the Au nanoparticle of the pattern. This indicates the successful binding of NTA-thiol, biomolecule, and primary and gold conjugated secondary antibodies. The diameter of the gold particle conjugated to the secondary antibody was approximately 5 nm and allows its distinction from the gold pattern which was made of 8 nm large dots. In Fig. 4(b), nearly each gold particle which forms the nanopattern carries two additional gold particles (yellow arrows) of 5 nm conjugated to the secondary antibody. This is very reasonable since in this study N-cadherins are homodimeric molecules. Only 1% of the Au nanoparticle of the pattern carried three additional nanoparticles. No Au nanoparticles of the pattern

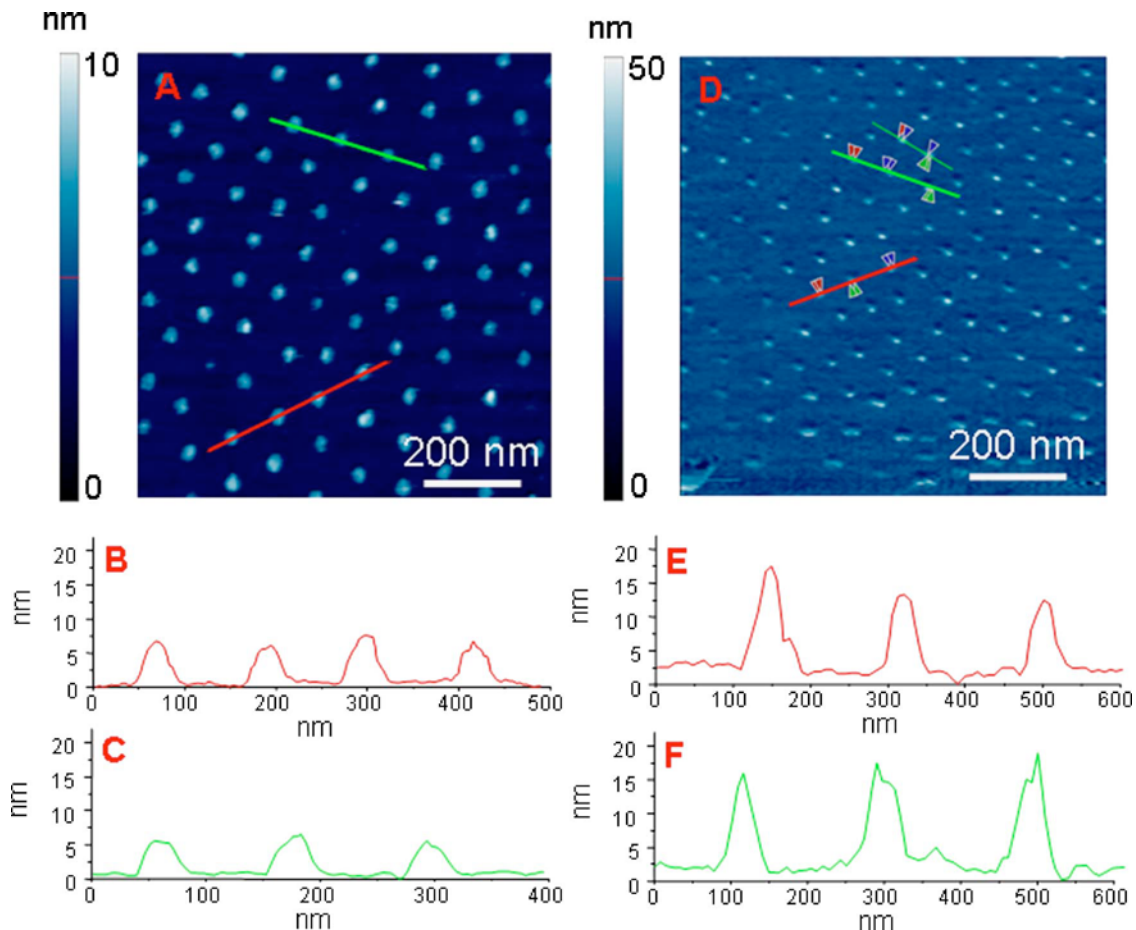


FIG. 3. (a) Scanning force microscopy analysis of NTA-thiol functionalized gold nanostructures. (b) and (c) display line analysis for these data as indicated by lines given in the image. (d) Scanning force microscopy analysis of N-cadherin functionalized gold nanoparticles. (e) and (f) show line analysis as indicated by lines given in (d).

were found that carried more than three additional gold particles. This proves that the size of the Au nanoparticle of the pattern restricts the number of homodimeric N-cadherin to up to 1. 24% of the Au nanoparticle of the pattern did not show additional gold particles to the one presented by the nanopattern. The reason for this might be manifold. N-cadherin located on the pattern might not be structurally active anymore, the secondary antibody did not carry a gold

particle, or the gold particle associated to the secondary antibody was located too close to the Au nanoparticle of the pattern such that SE microscopy could not resolve it. This argumentation leads to the conclusion that the successful binding of functional homodimeric N-cadherin might be substantially better than the given 75%.

In the case of agrin, detection of two conjugated gold particles per Au nanoparticle of the pattern [Fig. 4(c), yellow

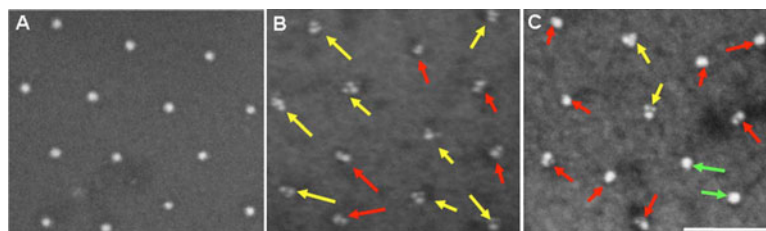


FIG. 4. Immunogold SE microscopy for detection of single molecules. (a) Negative control of N-cadherin functionalized nanopattern does not show unspecific binding of gold conjugated secondary antibodies if not treated with primary antibodies first. (b) N-cadherin and (c) agrin biofunctionalized nanostructures after incubation with respective monoclonal primary and gold conjugated secondary antibodies. Arrows indicate the location of two (yellow arrow) and one (red arrow) additional gold (5 nm) conjugated antibodies close to a gold particle (8 nm) which forms the nanopattern. Green arrows indicate location of gold particles conjugated to secondary antibodies on top of the gold from the nanopattern. These sites do not resolve a second spot but brighter intensity. Note that N-cadherin (b) is a homodimer providing two binding site for the monoclonal antibody, while agrin (c) is a monovalent biomolecule. Scale bar is 100 nm for all images.

arrows] was found for 57% out of 830 cases. Principally gold labels conjugated to the secondary antibody seem to be closer to the Au nanoparticle of the pattern than for N-cadherin. This is also in consistence with SF-microscopy results for agrin on nanopatterns, showing less high objects than those for cadherin (data not shown). In a few cases, gold labels seem to be on top of a gold dot from the pattern since these dots are stronger in intensity than nonlabeled gold dots from the pattern [Fig. 4(c), green arrows]. These were also counted as a successful binding event. However, resolving of the second gold particle is much harder for agrin patterns because of the smaller size of the protein which resulted in 38% of the Au nanoparticle of the pattern to appear not labeled. Only 5% of the Au nanoparticle of the pattern carried two gold particles from the antibody. No event was found where more than two gold particles per pattern dot were found. Again this proves that the size of the Au nanoparticle from the pattern restricts the number of functional agrin molecules up to 1.

IV. CONCLUSION

The results show that up to 75% of gold particles which form the nanopattern are covered with only a single functional biomolecule, i.e., N-cadherin. The precision given by such surface concentrations are much higher than in any other cases reported so far. In addition, the data prove that the given density is molecularly defined. This is an essential requirement for the control of functional biomolecule clustering since many biomolecules operate not as individual entities but rather as part of a macromolecular complex. Since the chemistry for attaching His tags to proteins is very general, this approach enables the application of a large number of different biomolecules oriented in a nanoscaled array. Such arrays of single biomolecules can be applied in cell culture studies, presenting a molecularly defined environment to cell surfaces. Especially transmembrane proteins with relevance for cell adhesion, survival, and differentiation are interesting candidates for those substrates. Such nanopattern substrates offer for the first time investigations with respect to the function of single molecules arranged in molecularly defined pattern. One can exactly determine the number, spatial positioning, and orientation of molecules being presented at the interface.

ACKNOWLEDGMENTS

The authors are thankful to Jacques Blümmel for synthesizing mPEG-triethoxysilanes. The authors thank J. Bewersdorf, W. Eck, and M. Schmitt for helpful discussions. The scanning force measurements were performed in the laboratory of S. Collins, University of Maine. This work was supported by the EU-IP NanoEar Programme (Project Number 026556), Alfried Krupp von Bohlen und Halbach-Stiftung, National Science Foundation, and the Max-Planck-Society.

- ¹D. L. Spector, R. D. Goldman, and L. A. Leinwand, *Cells: A Laboratory Manual* (CSHL, 1998).
- ²L. L. Kiessling, J. E. Gestwicki, and L. E. Strong, *Angew. Chem., Int. Ed.* **45**, 2348 (2006).
- ³M. Arnold, E. A. Cavalcanti-Adam, R. Glass, J. Blummel, W. Eck, M. Kantlehner, H. Kessler, and J. P. Spatz, *ChemPhysChem* **19**, 383 (2004).
- ⁴E. A. Cavalcanti-Adam, A. Micoulet, J. Blummel, J. Auernheimer, H. Kessler, and J. P. Spatz, *Eur. J. Cell Biol.* **85**, 219 (2006).
- ⁵M. A. Cooper, *Nat. Rev. Drug Discovery* **1**, 515 (2002).
- ⁶N. Green, *Avidin and Streptavidin, Avidin-Biotin Technology, Methods in Enzymology*, (Academic, San Diego, 1990).
- ⁷J. Groll, K. Albrecht, P. Gasteier, S. Riethmueller, U. Ziener, and M. Moeller, *ChemBioChem* **6**, 1782 (2005).
- ⁸G. Lemercier and K. Johnsson, *Nat. Methods* **3**, 247 (2006).
- ⁹G. B. Sigal, C. Bamdad, A. Barberis, J. Strominger, and G. M. Whitesides, *Anal. Chem.* **68**, 490 (1996).
- ¹⁰K. Ataka, F. Giess, W. Knoll, R. Naumann, S. Haber-Pohlmeier, B. Richter, and J. Heberle, *J. Am. Chem. Soc.* **126**, 16199 (2004).
- ¹¹L. Nieba *et al.*, *Anal. Biochem.* **252**, 217 (1997).
- ¹²J. Schmitt, H. Hess, and H. G. Stunnenberg, *Mol. Biol. Rep.* **18**, 223 (1993).
- ¹³P. Hintendorfer and Y. F. Dufrene, *Nat. Methods* **3**, 347 (2006).
- ¹⁴S. Lata, M. Gavutis, R. Tampe, and J. Piehler, *J. Am. Chem. Soc.* **128**, 2365 (2006).
- ¹⁵D. L. Johnson and L. L. Martin, *J. Am. Chem. Soc.* **127**, 2018 (2005).
- ¹⁶V. N. Truskett and M. P. Watts, *Trends Biotechnol.* **24**, 312 (2006).
- ¹⁷M. L. Dustin and D. R. Colman, *Science* **298**, 785 (2002).
- ¹⁸B. F. Lillemeier, J. R. Pfeiffer, Z. Surviladze, B. S. Wilson, and M. M. Davis, *Proc. Natl. Acad. Sci. U.S.A.* **103**, 18992 (2006).
- ¹⁹G. A. Silva, *Nat. Rev. Neurosci.* **7**, 65 (2006).
- ²⁰K. Busch and R. Tampe, *Mol. Biotechnol.* **82**, 3 (2001).
- ²¹J. Spatz *et al.*, *Langmuir* **16**, 407 (2000).
- ²²R. Glass, M. Moeller, and J. P. Spatz, *Nanotechnology* **14**, 1153 (2003).
- ²³G. Kadmon and P. Altevogt, *Differentiation* **61**, 143 (1997).
- ²⁴G. Tsen, W. Halfter, S. Kroger, and G. J. Cole, *J. Biol. Chem.* **270**, 3392 (1995).
- ²⁵M. Takeichi, *Curr. Opin. Cell Biol.* **7**, 619 (1995).
- ²⁶U. Tepass, K. Truong, D. Godt, M. Ikura, and M. Peifer, *Nat. Rev. Mol. Cell Biol.* **1**, 91 (2000).